



ELSEVIER

Available online at www.sciencedirect.com

SCIENCE @ DIRECT®

Journal of Sound and Vibration 291 (2006) 169–191

JOURNAL OF
SOUND AND
VIBRATION

www.elsevier.com/locate/jsvi

Fatigue lifetime estimation of commercial vehicles

Mario Leonardo Boéssio^a, Inácio Benvegno Morsch^{b,*},
Armando Miguel Awruch^b

^a*Technical Course in Industrial Mechanics, Federal Center of Technological Education of Rio Grande do Sul – CEFET-RS, Praça Vinte de Setembro, 455, 96015-360, Pelotas, RS, Brazil*

^b*Department of Civil Engineering, Federal University of Rio Grande do Sul, Av. Osvaldo Aranha, 99 – 3° Andar, 90035-190, Porto Alegre, RS, Brazil*

Received 1 July 2004; received in revised form 9 May 2005; accepted 1 June 2005

Available online 19 August 2005

Abstract

A computational procedure for the analysis and design of commercial vehicles structures is the main objective of this work. Random fatigue analysis due to the effect of rough pavement surfaces is carried out in the time domain based on Wöhler's curves (stress levels vs. number of cycles), the Palmgreen–Miner's rule to compute the cumulative damage and the rainflow method for cycles counting. First-order reliability method (FORM) and Monte Carlo simulation with importance and adaptive sampling (MCSIAS) are used to evaluate the reliability index, which may be employed as a constraint in the weight optimization process. The structural weight optimization is performed using Farkas' method with discrete variables.

© 2005 Elsevier Ltd. All rights reserved.

1. Introduction

A computational algorithm for the fatigue analysis and design of commercial vehicles structures using a simplified model with spatial frame bars is the main goal of this work. The aim of the computational procedure presented here is to obtain more realistic design criteria than those usually employed by industrial design practice.

*Corresponding author. Tel.: +55 51 3316 3463; fax: +55 51 3316 3999.
E-mail address: morsch@cpgec.ufrgs.br (I.B. Morsch).

This model involves several topics, such as the following:

- (a) Static analysis due to the structural weight and the effects of baggages and passengers.
- (b) Dynamic analysis in the time domain of a vehicle travelling on rough pavements surfaces. As these surfaces are random fields, they must be characterized by statistical quantities, such as the mean value, the variance and the power spectral density function. Then, the corresponding dynamic problem is a random process with support excitation. In this work, the pavement surface is considered as a two-dimensional Gaussian, isotropic and homogeneous random field. Although spectral density functions for different states of pavements surfaces were presented by several authors, such as Dodds and Robson [1] and Ashmore and Hodges [2], here the first one was adopted. The dynamic equilibrium equation of the system, expressed in matrix form, is based on the approach presented in Ref. [3] with some modifications, and the numerical solution is obtained using Newmark's implicit method [4], and samples of the prescribed displacement at the contact points between the vehicle and the road in the time domain may be obtained with the pavement surface spectral density function and a harmonic series, as indicated by Wirsching [5].
- (c) A procedure to evaluate the vehicle lifetime. The vehicle is subjected to random multiaxial fatigue. Although several sophisticated models for fatigue analysis exist, the Palmgreen–Miner rule to determine the vehicle lifetime due to fatigue was adopted. This model, as well as several other methods for fatigue analysis are described in Ref. [6].
- (d) Reliability analysis to evaluate the system failure probability. Considering uncertainties with respect to several parameters such as the variability of material properties values, dimensions of structural members and the process involving material fatigue, a failure probability (or reliability index) may be determined in order to guarantee a specified safety level to the structural system. In this work, classical techniques, such as the first-order reliability method (FORM), described, for example, by Haldar and Mahadevan [7] and Monte Carlo simulation with importance and adaptive sampling (MCSIAS), were used [8–13].
- (e) Application of an optimization technique to minimize the structural weight subject to constraints based on yield stress, members stability and lifetime associated with failure probability. In this work, the Farkas' method [14], using discrete variables, was adopted.

Finally, the computational code was applied to a simplified model representing a bus, with structural dimensions and loads similar to those used in this type of vehicles.

2. Formulation of the structural dynamic problem

2.1. The dynamic equilibrium equation

The rough pavement surfaces induce random loads on the structure, generating varying stress components in the time domain that may lead to a fatigue failure process. This criterion defines the vehicle lifetime. However, as a preliminary design, static analysis must also be carried out, taking into account loads due to the structural weight and the effects of passengers and baggage.

The dynamic equilibrium equation of the vehicle is given by

$$\begin{bmatrix} \mathbf{M}_{cc} & \mathbf{M}_{cb} \\ \mathbf{M}_{bc} & \mathbf{M}_{bb} \end{bmatrix} \cdot \begin{bmatrix} \ddot{\mathbf{u}}_c \\ \ddot{\mathbf{u}}_b \end{bmatrix} + \begin{bmatrix} \mathbf{C}_{cc} & \mathbf{C}_{cb} \\ \mathbf{C}_{bc} & \mathbf{C}_{bb} \end{bmatrix} \cdot \begin{bmatrix} \dot{\mathbf{u}}_c \\ \dot{\mathbf{u}}_b \end{bmatrix} + \begin{bmatrix} \mathbf{K}_{cc} & \mathbf{K}_{cb} \\ \mathbf{K}_{bc} & \mathbf{K}_{bb} \end{bmatrix} \cdot \begin{bmatrix} \mathbf{u}_c \\ \mathbf{u}_b \end{bmatrix} = \begin{bmatrix} 0 \\ 0 \end{bmatrix}, \quad (1)$$

where \mathbf{M}_{cc} , \mathbf{C}_{cc} and \mathbf{K}_{cc} are, respectively, the mass, damping and stiffness matrices of the chassis and the body. \mathbf{M}_{bb} , \mathbf{C}_{bb} and \mathbf{K}_{bb} are the mass, damping and stiffness matrices of the suspension. Terms coupling effects of chassis, body and suspension are indicated in Eq. (1) with the index cb or bc . The absolute displacement components are contained in vector \mathbf{u}_c , which corresponds to the unrestrained degrees of freedom of the chassis and the body. Prescribed displacement components in points where the vehicle contacts the road surface are contained in \mathbf{u}_b .

From Eq. (1), the following equations may be written:

$$\mathbf{M}_{cc}\ddot{\mathbf{u}}_c + \mathbf{C}_{cc}\dot{\mathbf{u}}_c + \mathbf{K}_{cc}\mathbf{u}_c = -\mathbf{M}_{cb}\ddot{\mathbf{u}}_b - \mathbf{C}_{cb}\dot{\mathbf{u}}_b - \mathbf{K}_{cb}\mathbf{u}_b \quad (2)$$

and

$$\mathbf{M}_{bc}\ddot{\mathbf{u}}_c + \mathbf{C}_{bc}\dot{\mathbf{u}}_c + \mathbf{K}_{bc}\mathbf{u}_c = -\mathbf{M}_{bb}\ddot{\mathbf{u}}_b - \mathbf{C}_{bb}\dot{\mathbf{u}}_b - \mathbf{K}_{bb}\mathbf{u}_b. \quad (3)$$

Multiplying Eq. (3) by $-\mathbf{M}_{cb}\mathbf{M}_{bb}^{-1}$, and adding each term of this expression to Eq. (2), the following equation is obtained:

$$\begin{aligned} & -\mathbf{M}_{cb}\mathbf{M}_{bb}^{-1}\mathbf{M}_{bc}\ddot{\mathbf{u}}_c - \mathbf{M}_{cb}\mathbf{M}_{bb}^{-1}\mathbf{C}_{bc}\dot{\mathbf{u}}_c - \mathbf{M}_{cb}\mathbf{M}_{bb}^{-1}\mathbf{K}_{bc}\mathbf{u}_c \\ & = +\mathbf{M}_{cb}\mathbf{M}_{bb}^{-1}\mathbf{M}_{bb}\ddot{\mathbf{u}}_b + \mathbf{M}_{cb}\mathbf{M}_{bb}^{-1}\mathbf{C}_{bb}\dot{\mathbf{u}}_b + \mathbf{M}_{cb}\mathbf{M}_{bb}^{-1}\mathbf{K}_{bb}\mathbf{u}_b. \end{aligned} \quad (4)$$

Assuming that the mass matrices of the suspension elements are diagonal matrices, $\mathbf{M}_{cb} = 0$ and $\mathbf{M}_{bc} = 0$. Then, Eq. (4) may be written as follows:

$$\mathbf{M}_{cc}\ddot{\mathbf{u}}_c + \mathbf{C}_{cc}\dot{\mathbf{u}}_c + \mathbf{K}_{cc}\mathbf{u}_c = -\mathbf{C}_{cb}\dot{\mathbf{u}}_b - \mathbf{K}_{cb}\mathbf{u}_b. \quad (5)$$

Expressions given by Eq. (4) or by Eq. (5) may be solved using Newmark's method [4].

2.2. Description of the rough pavement surfaces and determination of the prescribed displacement samples

Pavement surfaces are represented by a random two-dimensional isotropic Gaussian field in this work. The model of the spectral density function, proposed by Dodds and Robson [1], was adopted and it is given by:

$$G(n) = cn^{-w}, \quad (6)$$

where n is the wavenumber, w is a constant value (usually $w = 2.5$) and c depends on the state of the road surface. Values of c were presented by Dodds and Robson [1] and they vary from 2×10^{-8} to 3×10^{-5} . The wavenumber n is related to the angular frequency ω and the vehicle velocity V by the expression $\omega = 2\pi nV$. Eq. (6) is valid for values of frequencies ranging from 0.5 to 50 Hz, and velocities varying from 5 to 50 m/s. These frequency and velocity intervals correspond to values of wavenumbers varying between 0.1 and 10 cycles/m.

Once the spectral density function $G(n)$ (or $G(\omega)$), which is a function of the vehicle velocity, is known, the displacements are obtained with the following expression:

$$u_{mi}(t) = \sum_{k=1}^M [2G(\omega_k)\Delta\omega_k]^{1/2} \cos(\omega_k t + \phi_k), \quad (7)$$

where m and i indicate the input number and the sample number, M is the number of harmonic components, $\Delta\omega_k$ is the length of a specific angular frequency interval, ϕ_k is the phase angle and $(G\omega_k)$ gives the value of the spectral density function for a specific value $\omega_k \geq 0$ of the angular frequency. As suggested by Wirsching [5], the phase angle ϕ_k was considered as a random variable, with uniform distribution in the interval $(0, 2\pi)$. In order to avoid sampling periodicity, the frequency interval $\Delta\omega_k$ was also considered as a random variable. Although representation of the pavement surface as an isotropic model could be considered as a simplified model, it is very difficult to get available data to use more complex representations, including correlation coefficients and singularities, such as holes located in specific regions of the road.

3. Multiaxial random fatigue

3.1. State of stress

Stress components are calculated using classical strength of materials theory. They are computed in each step, during the solution process of the dynamic problem, at some points of the cross section. Different types of cross sections used in this work, as well as points where stresses are calculated, can be observed in Fig. 1, where end forces are also shown.

In each point at the cross section, histories of the normal stress σ_{xx} and the shear stress τ_{xy} are obtained. These two histories do not present any direct correspondence in terms of peaks and valleys. This aspect is very important to define a criterion for cycles counting and their combined effects. It may be observed that the dynamic problem is a random process and concepts such as periodicity and synchronism cannot be applied. Maximum and minimum values of normal and shear stresses are obtained in each point using the cycles counting process. In this work the rainflow method [6] was used.

3.2. Cumulative damage and lifetime estimate

In this work, a high cycle fatigue problem is considered. Therefore, the lifetime is estimated by the stress-life approach, while the cumulative damage is calculated using the Palmgreen–Miner rule.

When data for a specific material are not available, “*stress level vs. number of cycles*” curves may be approximated. In this work, the high cycle fatigue regime is initiated at 1×10^3 cycles and the corresponding stress σ_{10^3} may be obtained with the Manson expression [15] ($\sigma_{10^3} = 0.9\sigma_r$), where σ_r is the ultimate stress.

In commercial vehicle body structures, where steel with low grade of carbon is usually employed, the yield stress is approximately equal to 250 MPa and the fatigue limit, for 10^6 cycles, may be approximate by $\sigma_{\text{ftb}} = 0.5\sigma_r$, where σ_{ftb} is the fatigue limit of a standard test body. For

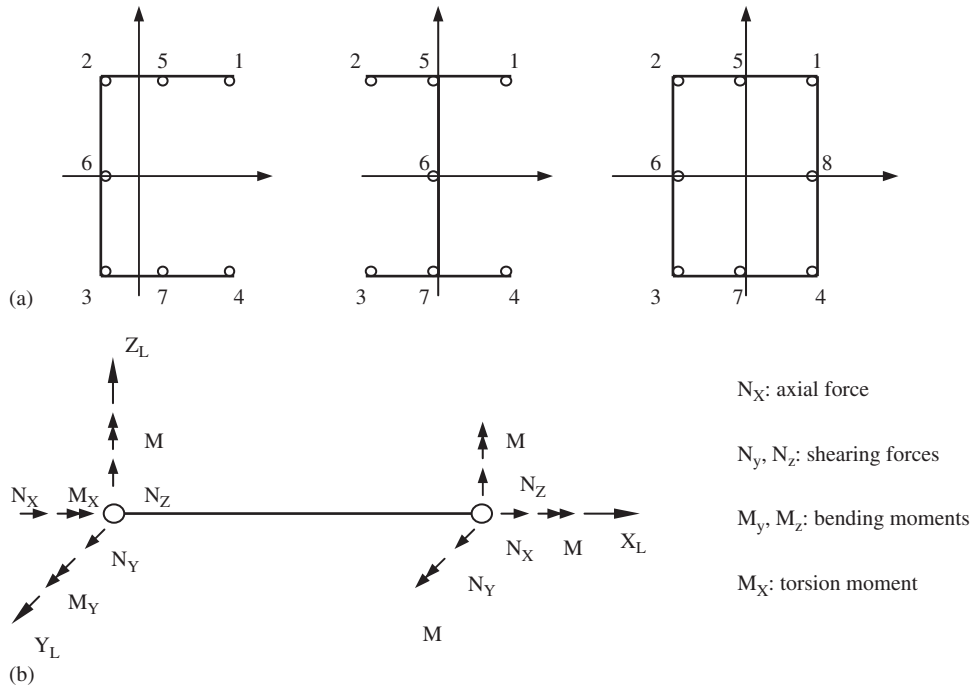


Fig. 1. (a) Points of different cross sections where stress components are verified; (b) end forces acting on each element of the space frame.

structural members, this value must be corrected, using the following expression:

$$\sigma_f = K_a K_b K_{\text{weld}} 0.5 \sigma_r, \tag{8}$$

where K_a is the surface factor, K_b is the size factor and K_{weld} is the weld factor. These coefficients were used by several authors such as Norton [15], Juvinall [16] and Shigley [17]. Values adopted for these three coefficients will be presented in the numerical application.

Fatigue curves may be expressed by the following analytical equation:

$$N \sigma^m = K = 10^a \quad \text{for} \quad 10^3 \leq N \leq 10^6, \tag{9}$$

where coefficients m and a may be obtained by experimental tests. This standard curve is valid in the interval between 10^3 and 10^6 cycles. A cut-off limit given by

$$\log \sigma_f = \text{constant} \quad \text{for} \quad N > 10^6 \text{ cycles} \tag{10}$$

is adopted. Below this stress level, there is no structural damage due to material fatigue.

Eqs. (9) and (10) are represented by curve A in Fig. 2.

When loads have variable amplitude in welded metal structures, a stress level less than the fatigue limit may produce crack propagation causing damage. To take into account this problem, the EUROCODE 3 [18] extends the interval of Eq. (9) until $N = 5 \times 10^6$ cycles, and then a new segment, valid in the interval between 5×10^6 and 10^8 cycles, is adopted, whose

equation is given by:

$$N\sigma^{m+2} = K = 10^a \quad \text{for} \quad 5 \times 10^6 \leq N \leq 10^8. \tag{11}$$

The last part of the curve, adopted by the EUROCODE 3 for $N > 10^8$ cycles, is

$$\log \sigma_f = \text{constant} \quad \text{for} \quad N > 10^8. \tag{12}$$

Eqs. (9), (11) and (12) are represented by curve B in Fig. 2. Finally, another procedure may be used, extending the curve given by Eq. (9) until the horizontal axis, as indicated by curve C in Fig. 2.

The classical Palmgreen–Miner rule was adopted to calculate the cumulative damage, which is given by

$$\Delta \geq \sum_{i=1}^k \frac{n_i}{N_i} = D, \tag{13}$$

where k is the number of the different stress levels, n_i is the number of cycles for the stress level i , N_i is the fatigue lifetime for the stress level i , D is the cumulative damage and Δ is the limit value of the cumulative damage. When fatigue failure occurs, Δ assumes values varying between 0.3 and

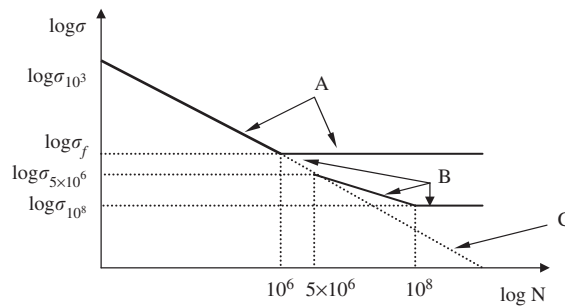


Fig. 2. Curves “stress level vs. number of cycles”: (A) standard curve; (B) curve given by EUROCODE 3; (C) Eq. (11) extended until the horizontal axis.

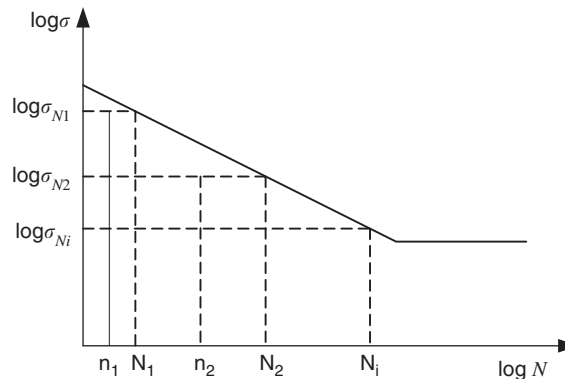


Fig. 3. Evaluation of the damage components for different stress levels.

3.0, depending on several factors with random characteristics [15]. Components of the sum indicated in Eq. (13) may be observed in Fig. 3.

Effects of the mean value of the alternating stresses must be taken into account. In this work the expression given by Goodman [6] is used to obtain an equivalent stress (with a complete reverse cycle), considering the influence of the mean value, and may be written as

$$\sigma_{\text{equiv}} = \frac{\sigma_a}{(1 - \sigma_m/\sigma_r)}, \quad (14)$$

where σ_{equiv} is the equivalent stress, σ_a is the alternating stress, σ_m is the mean value of the alternating stress and σ_r is the ultimate stress.

Taking into account Eqs. (9) and (13), the Palmgreen–Miner rule may be expressed in the following form:

$$D = \frac{1}{2} \sum_{i=1}^{n_c} \frac{(\sigma^m)_i}{K}, \quad (15)$$

where D is the damage and n_c is the number of half cycles determined by the rainflow method.

3.3. Criteria for a multiaxial state stress

For a multiaxial state of stress, cycles counting requires special considerations, depending on the method or the code that will be used. In some cases, cycles counting is carried out taking into account the history of each stress component separately. In other cases, cycle counting is performed combining histories of the different stress components.

Three procedures may be adopted: (a) Shigley's method [17], (b) EUROCODE 3 [18] and (c) Sines' method.

In Shigley's method equivalent stress components, alternating stress components and mean value of the alternating stress components, used in Eq. (14), are computed using the equivalent von Mises criterion. It is necessary to point out that positive and negative values of normal and shear stress components in the records may be lost due to stress combination. In this work, it was considered that the von Mises equivalent stress has the same sign as the predominant stress component. After filtering and counting, each cycle is transformed in a completely reversed cycle and the corresponding damage is calculated.

The EUROCODE 3 suggests, for the case of variable stress, that the cumulative damage may be computed separately for the normal and the shear stresses. Then, the total cumulative damage is calculated by the sum of the cumulative damage determined for each stress component separately.

Sines' method is similar to Shigley's method, but it does not consider the influence of the mean value of the alternating shear stress, and then the equivalent mean value of the alternating stress is given only by the effects of the normal stress.

In the computer code, the procedures suggested by Shigley and by EUROCODE 3 were included, but the effect of the mean value of the alternating shear stress as indicated by Sines [19] may be neglected.

3.4. Computational procedure for the dynamic and fatigue analysis

The computational procedure to evaluate the structural lifetime due to material fatigue is summarized in the following steps:

- (1) input data corresponding to the structure and the pavement. Data to perform simulations in the time domain must be also given;
- (2) assembling, application of the boundary conditions and decomposition of the coefficient matrix, which is a function of the mass, damping and stiffness matrices, are carried out;
- (3) initiate a loop for $i = 1$ until the number of different conditions in which the vehicle will work, characterized by the vehicle velocity levels and respective pavement roughness during the lifetime;
- (4) generate the effects of the pavement roughness samples through the phase angle. Initiate a loop for $j = 1$ until the number of samples;
- (5) initiate a loop for $k = 1$ until the number of time intervals;
- (6) assembling, application of the boundary conditions to the load vector and back substitution to obtain displacement components are performed;
- (7) calculate efforts and stress components of structural members;
- (8) end of the loop for k ;
- (9) fatigue analysis: for a uniaxial state of stress, normal stresses are used; for a biaxial state of stress, Shigley's method [17] (using the von Mises equivalent stress) or the EUROCODE 3 [18] with the suggestion given by Sines (neglecting effects of the mean value of the shear stress) may be used; store stress obtained for each sample of the pavement surface.
- (10) end of the loop for j ;
- (11) calculate the structure lifetime;
- (12) end of the loop for i .

4. Structural reliability analysis

4.1. The failure probability

Evaluation of the failure probability and safety levels of structural systems is of extreme importance in structural design, mainly when variables are eminently random. Random variables, such as material properties, loads and member dimensions, are physical uncertainties and it is necessary to quantify and compare the importance of each one of these variables in the structural safety.

As it is very difficult to take into account all kinds of uncertainties (including those due to human factors, phenomenological aspects or due to the adopted model), the failure probability (or its complement, the reliability index) may be thought of as a “formal” quantity which has some meaning when it is a result of comparisons with reliability evaluations of structural systems, where the same uncertainties have been adopted. In this way, structural reliability arises as an important tool to compare existing structural design procedures and to validate design rules established in the corresponding practice codes.

For structural reliability analysis, the structural characteristics may be defined by a vector of basic random variables \mathbf{X} . In order to compute the failure probability it is necessary to formulate a limit state function $g(\mathbf{X})$ such that $g(\mathbf{X}) > 0$ when safety conditions are satisfied and the corresponding point in the space generated by the components of the vector \mathbf{X} is located in the safety region. On the other hand, if $g(\mathbf{X}) \leq 0$, then the design requirements are not satisfied and the corresponding point is located in the failure region of the variable space. The failure probability P_f is given by

$$P_f = \int_{[g(\mathbf{X}) \leq 0]} f_{\mathbf{x}}(\mathbf{X}) d\mathbf{X}, \tag{16}$$

where $f_{\mathbf{x}}(\mathbf{X})$ is the joint probability density function of the random variables. Evaluation of Eq. (16) is very difficult because sometimes $f_{\mathbf{x}}(\mathbf{X})$ is not known and for completely general limit state functions in large dimension spaces it demands a tremendous task. There are several classical techniques to evaluate P_f or its complement, the reliability index β . FORM and MCSAIS were used in this work.

4.2. FORM

FORM is an optimization problem, which may be stated as follows:

$$\text{Minimize } \beta = \|\mathbf{Z}\|, \quad \text{subject to } G(\mathbf{Z}) = 0, \tag{17}$$

where β is the reliability index, \mathbf{Z} is the vector of variables in the non-correlated standard Gaussian space, $G(\mathbf{Z})$ is the limit state function, transformed to the non-correlated Gaussian space and the symbol $\|\cdot\|$ indicates the Euclidian norm. The corresponding result is the smallest distance β from the origin of the reference system in the variable space to the limit state function. The point of intersection between the vector \mathbf{Z} of magnitude β and the surface $G(\mathbf{Z}) = 0$ is the design point, and the corresponding coordinate is contained in vector \mathbf{Z}^* .

Variables in the non-correlated standard Gaussian space are related to variables in the real space (which may be a non-Gaussian space), with coordinates contained in vector \mathbf{X} and a limit state function $g(\mathbf{X})$, by the probabilistic transformation

$$\mathbf{Z} = S(\mathbf{X}) = L^{-1} \Phi^{-1} F_{\mathbf{X}}(\mathbf{X}) \quad \text{or} \quad \mathbf{X} = T(\mathbf{Z}) = S^{-1}(\mathbf{Z}), \tag{18}$$

where L^{-1} is the inverse of the lower triangular matrix resulting from the Choleski decomposition of $\boldsymbol{\rho}'$, which is the matrix of the correlation coefficients in the standard Gaussian space; Φ^{-1} the inverse of the standard Gaussian cumulative probability function; $F_{\mathbf{X}}$ the Cumulative probability function in the real space. If \mathbf{X} is a correlated standard Gaussian space $F_{\mathbf{X}} = \Phi$.

Terms of matrix $\boldsymbol{\rho}'$ may be obtained from the matrix of correlation coefficients in the real space $\boldsymbol{\rho}$ using Nataf's model [20], which is given by

$$\rho_{ij} = \int_{-\infty}^{\infty} \int_{-\infty}^{\infty} \left(\frac{x_i - \mu_i}{\psi_i} \right) \left(\frac{x_j - \mu_j}{\psi_j} \right) \varphi(z_1, z_2, \rho'_{ij}) dz_i dz_j, \tag{19}$$

where $\mu_i, \mu_j, \psi_i,$ and ψ_j are the mean values and standard deviations of variables z_i and z_j , respectively, and $\varphi(z_1, z_2, \rho'_{ij})$ is the two-dimensional standard Gaussian probability density function (with mean values equal to zero and standard deviations equal to one).

Elements of matrix $\boldsymbol{\rho}$ may be calculated using exponential, square exponential or sinusoidal correlation. After elements ρ_{ij} in the real space have been calculated, terms ρ'_{ij} in the standard Gaussian space can be calculated by numerical integration of Eq. (19) or by empirical expressions (see Ref. [20]). If \mathbf{X} is in the correlated standard Gaussian space, then Nataf's model is not used, and $\rho'_{ij} = C_{X_{ij}}/\psi_i\psi_j$, where $C_{X_{ij}}$ is an element of the covariance matrix (which can be obtained with the mean values μ_i and μ_j).

The computational procedure for the reliability analysis of structures using FORM can be summarized in the following steps [21]:

- (1) Set k (iteration counter) = 0.
- (2) Perform the finite element analysis of the structural system. To start the iterative process the initial value $\mathbf{Z}_0 = \mathbf{0}$ is adopted, which corresponds to a vector \mathbf{X}_0 containing the mean values of the variables in the real space. The limit state function $g(\mathbf{X}_k)$ is obtained.
- (3) Compute the limit state function $G(\mathbf{Z}_k)$ in the non-correlated standard Gaussian space, which is given by $G(\mathbf{Z}_k) = G[S(\mathbf{X}_k)] = g(\mathbf{X}_k)$.
- (4) Compute the gradient $\nabla G(\mathbf{X}_k)$.
- (5) Set k (iteration counter) = $k + 1$. Using the method of Hasofer–Lind (H–L method) and the method of Rackwitz–Fiessler (see Ref. [7]), compute

$$\mathbf{Z}_{k+1} = \mathbf{Z}_k + s\mathbf{d}_k, \quad (20)$$

where s is a parameter defining the step length and \mathbf{d}_k is a direction-searching vector calculated with the following expression:

$$\mathbf{d}_k = \frac{1}{\|\nabla G(\mathbf{Z}_k)\|} [\mathbf{Z}_k^T \cdot \nabla G(\mathbf{Z}_k) - G(\mathbf{Z}_k)] \nabla G(\mathbf{Z}_k) - \mathbf{Z}_k. \quad (21)$$

- (6) Calculate

$$m(\mathbf{Z}_k) = \frac{1}{2} \left\| \mathbf{Z}_k - \frac{\nabla G(\mathbf{Z}_k)^T \cdot \mathbf{Z}_k}{\|\nabla G(\mathbf{Z}_k)\|^2} \nabla G(\mathbf{Z}_k) \right\|^2 + \frac{1}{2} \hat{c} [G(\mathbf{Z}_k)^2] \geq 0, \quad (22)$$

where \hat{c} is a positive constant (usually $\hat{c} = 0.1$). The function $m(\mathbf{Z}_k)$ must decrease in each iteration, such that a global minimum value is obtained when $\mathbf{Z}_k = \mathbf{Z}^*$ (\mathbf{Z}^* is the design point). Different values of s (step length) are used, computing \mathbf{d}_k with Eq. (21), \mathbf{Z}_{k+1} with Eq. (20) and $m(\mathbf{Z}_k)$ with Eq. (22). When $m(\mathbf{Z}_{k+1}) < m(\mathbf{Z}_k)$ is satisfied, the value of s is found.

- (7) Compute the reliability index $\beta = \|\mathbf{Z}_{k+1}\|$ and the failure probability $P_f = \Phi(-\beta)$, where $\Phi(\cdot)$ is the standard Gaussian cumulative probability function.
- (8) Compute \mathbf{Z}'_{k+1} , the vector of variables, in the correlated Gaussian space and \mathbf{X}_{k+1} in the real space using

$$\mathbf{Z}'_{k+1} = \mathbf{L}\mathbf{Z}_k \quad \text{and} \quad \mathbf{X}_{k+1} = F_X^{-1}[\Phi(\mathbf{Z}'_{k+1})] = F_X^{-1}[\Phi(\mathbf{L}\mathbf{Z}_{k+1})] = T(\mathbf{Z}_{k+1}). \quad (23)$$

- (9) Check the convergence of \mathbf{Z}_{k+1} and check if $G(\mathbf{Z}_{k+1}) \cong 0$. If convergence is not satisfied, go back to step (2), else stop the iterative process, and set $\mathbf{Z}^* = \mathbf{Z}_{k+1}$. Sensitivity of β may be optionally calculated in the real space.

4.3. Monte Carlo simulation with importance sampling

Basically, the Monte Carlo method consists in the simulation of a large number of experiments generated in an artificial form. These experiments are samples of the random variables \mathbf{X} , and after their generation the limit state function $g(\mathbf{X})$ is evaluated. Then, this method may be understood as the relative frequency of the failure cases (when $g(\mathbf{X}) < 0$) observed in the different samples.

The computational procedure for the reliability analysis using the Monte Carlo method can be summarized in the following steps:

- (1) initiate a loop for $k = 1$ until ns (number of simulations);
- (2) generate random numbers contained in vector \mathbf{u} , uniformly distributed between 0 and 1;
- (3) generate the vector of variables $\mathbf{Z}_k = \Phi^{-1}(\mathbf{u}_k)$ in the non-correlated standard Gaussian space, where $\Phi(\cdot)$ is the standard Gaussian cumulative probability function;
- (4) calculate \mathbf{Z}'_k in the correlated standard Gaussian space and \mathbf{X}_k in the real space with Eq. (23).
If \mathbf{X}_k is in the correlated standard Gaussian space, $\mathbf{X}_k = \mathbf{Z}'_k$;
- (5) perform the structural analysis and determine the limit state function $g(\mathbf{X}_k)$;
- (6) calculate:

$$I[g(\mathbf{X}_k)] = \begin{cases} 1 & \text{if } g(\mathbf{X}_k) \leq 0 \rightarrow \text{failure,} \\ 0 & \text{if } g(\mathbf{X}_k) > 0 \rightarrow \text{safety;} \end{cases} \quad (24)$$

- (7) calculate the partial value of the failure probability $P_{f_k} = P_{f_{k-1}} + (1/ns)I[g(\mathbf{X}_k)]$.
End of the loop. When $k = ns$, the failure probability is determined with the following expression:

$$P_f = \int_{[\mathbf{x}|g(\mathbf{x}) \leq 0]} f_{\mathbf{x}}(\mathbf{X})d\mathbf{X} = \int_{\mathbf{X}} I[g(\mathbf{X})]f_{\mathbf{x}}(\mathbf{X})d\mathbf{X} = \frac{1}{ns} \sum_{k=1}^{ns} I[g(\mathbf{X}_k)] = \mu_{P_f}; \quad (25)$$

- (8) calculate the standard deviation ψ_{P_f} and the variation coefficient δ_{P_f} with

$$\psi_{P_f} \cong \left[\frac{(1 - P_f)P_f}{ns} \right]^{1/2} \quad \text{and} \quad \delta_{P_f} = \frac{\psi_{P_f}}{\mu_{P_f}} \cong \left[\frac{(1 - P_f)}{nsP_f} \right]^{1/2} \quad (26)$$

- (9) if δ_{P_f} has no satisfactory value, then repeat steps (1)–(7), else determine the reliability index with $\beta = \Phi^{-1}(P_f)$.

In order to avoid an excessive number of simulations, it is convenient to use the Monte Carlo method with importance sampling. The basic idea of this technique consists in the concentration of the sample points in a region where they contribute more strongly to the failure probability. Then, sample points may be located near the design point.

When the importance sampling technique is used, the failure probability is calculated with the following expression, similar to Eq. (25):

$$P_f = \int_{\mathbf{X}} I_{\mathbf{w}}[g(\mathbf{X})]f_{\mathbf{w}}(\mathbf{X}) d\mathbf{X} = \frac{1}{ns} \sum_1^{ns} I_{\mathbf{w}}[g(\mathbf{X}_k)], \quad (27)$$

where $f_{\mathbf{w}}(\mathbf{X})$ is the sampling probability function and

$$I_{\mathbf{w}}[g(\mathbf{X})] = I[g(\mathbf{X})] \cdot \frac{f_{\mathbf{x}}(\mathbf{X})}{f_{\mathbf{w}}(\mathbf{X})}. \quad (28)$$

Some important characteristics of a good function $f_{\mathbf{w}}(\mathbf{X})$ are as follows:

- $f_{\mathbf{w}}(\mathbf{X})$ may be similar to $f_{\mathbf{x}}(\mathbf{X})$, but with its mean value moved in the direction of the failure domain;
- $f_{\mathbf{w}}(\mathbf{X})$ may be similar to $f_{\mathbf{x}}(\mathbf{X})$, but with an incremented standard deviation.

Function $f_{\mathbf{w}}(\mathbf{X})$ may be adapted during the process modifying the value of the standard deviation.

4.4. Structural reliability applied to analysis and design of vehicles structures

The limit state function (LSF) adopted in this work to carry out the reliability analysis is given by the following expression:

$$\text{LSF} = \text{LT} - \text{LT}_{\text{design}}, \quad (29)$$

where $\text{LT}_{\text{design}}$ is a constant representing the lifetime established for the structural design and LT is the lifetime, which is a function of random variables characterizing the material behavior subjected to fatigue.

The lifetime is obtained with the expression

$$\text{LT} = \frac{T}{D} \theta \Delta, \quad (30)$$

where T is the total time spent by each sample, D is the corresponding damage calculated with Eq. (15), Δ is given by Eq. (13) and θ is a random variable which is associated with the variation in the term $(\sigma^m)_i$ in Eq. (15), and defined in order to consider the variability of the lifetime estimation, as suggested by Wirsching [5].

It was mentioned previously that Δ may vary between 0.3 and 3.0 when fatigue failure occurs, and this value depends on factors with random characteristics [15]. For this reason Δ was taken as a random variable with a lognormal probability distribution function. The parameter K , in Eq. (17), was also taken as a random variable with lognormal probability distribution function.

The lognormal format was proposed by Wirsching [5] and Wirsching and Chen [22] as a convenient method to obtain a closed expression to evaluate the reliability index β . This is particularly useful when β is a constraint function of the weight optimization process, where the generation of design points with high values of lifetime may create numerical problems when FORM is employed.

When the failure probability is calculated using Monte Carlo simulation, Eq. (29) is used directly, but when FORM is employed, the limit state function may be written as follows:

$$g(\Delta, K) = \ln LT - \ln LT_{\text{design}}. \quad (31)$$

Applying Eqs. (13), (15) and (30), Eq. (31) is given by:

$$g(\Delta, K) = \ln \Delta + \ln K + \ln \theta + \ln LT + \ln 2 - \ln \left[\sum_i (\sigma_{vm}^m)_i \right] - \ln LT_{\text{design}}. \quad (32)$$

As Δ and K have a lognormal probability distribution, $\ln \Delta$ and $\ln K$ have a normal probability distribution. Applying FORM and using Eq. (32) as the limit state function, the following expression of the reliability index β is obtained:

$$\beta = \frac{\mu_{\ln LT} - \ln LT_{\text{design}}}{\psi_{\ln LT}}, \quad (33)$$

where $\mu_{\ln LT}$ and $\psi_{\ln LT}$ are the mean value and the standard deviation of $\ln LT$, respectively. This last value is given by

$$\psi_{\ln LT} = \left\{ \ln \left[(1 + C_k^2)(1 + C_\Delta^2)(1 + C_\theta^2) \right] \right\}^{1/2}, \quad (34)$$

where C_k , C_Δ and C_θ are the variation coefficients of the real variables K , Δ and θ , respectively.

5. The optimization procedure

In this work Farkas' method [14] for structural problems with discrete variables was adopted. In this method, design variables are discrete and the objective function is monotone in terms of these design variables.

The minimization problem is given by

$$\begin{aligned} & \text{Minimize } f(\mathbf{X}) \\ & \text{subject to } h_i(\mathbf{X}) \leq 0, \quad i = 1, \dots, m, \\ & \text{with } x_j \in (x_{j1}, x_{j2}, \dots, x_{jq}), \quad j = 1, \dots, n, \end{aligned} \quad (35)$$

where n is the number of variables, m is the number of constraints and q is the number of levels of each variable arranged in an ascending order. Levels may be represented, for example, by values of the cross section.

The basic steps are as follows:

- (1) The solution starts with all variables set at the highest level. The corresponding function value f_{\min} is an upper bound of $f(\mathbf{X})$ and \mathbf{X} is stored in \mathbf{X}_{\min} .
- (2) The variable levels are lowered one at a time successively, until x_{n-1} . Let us consider, for example, the first variable x_1 . Constraints are evaluated at level $l_1 = q$ and level $l_2 = 1$. If feasibility is satisfied at the lowest level l_2 , then the variable is set at that level and proceeds to the second variable. If level l_1 is feasible and level l_2 is not feasible, a new trial is set at the bisection point $l = \text{integer}(l_1 + l_2/2)$. If l is feasible, then l_1 is set equal to l , and set equal to l_2

otherwise. This process is continued until $l_1 - l_2 = 1$ and l_1 is the feasible level for x_1 . The same scheme is used for $x_2, \dots, x_{n-2}, x_{n-1}$. The process to determine the successively lowest level is called fathoming.

(3) The value of x_n is calculated determining the zero of the function $f(x_n) - f_{\min} = 0$.

The following situations may occur

- If x_n is larger than the highest value x_{n_q} (which is a feasible value), then the variable is decreased one step at a time until the lowest feasible level is identified. If $f(x_n) < f_{\min}$ (the previous bound of the objective function), then f_{\min} and \mathbf{X}_{\min} are updated. Fathoming has been completed, and the next step is initiated.
- If x_n is lower than the smallest value x_{n_1} , then the objective function value cannot be improved for this choice of levels. Fathoming has been completed, and the next step is initiated.
- If x_n lies between x_{n_1} and x_{n_q} , then constraints are evaluated at the next higher level and, if feasible, we go on to calculate at the next lower value. If this does not occur, the fathoming operation is stopped.

(4) A backtracking process is executed by increasing the previous variable x_{n-1} to the next higher level, and the next operation is the last variable check as described earlier in step (3). Whenever the level of another variable, x_{n-2} or below, is raised, the fathoming process, involving the bisection steps for variables up to $n-1$, is applied and then the last variable calculation is repeated as in step (3).

In this work, the aim is to minimize the structural weight. Consequently, the objective function is the total material volume, which is given by

$$f(A) = \sum_{i=1}^{\text{nb}} A_i l_i, \quad (36)$$

where nb is the number of bars, and A_i and l_i are their respective cross sections and lengths.

The constraints are referred to possible failure modes such as limit yield for stress, overall buckling of bars, local buckling in thin-walled structural members and a reliability index for the probabilistic fatigue analysis.

To verify yielding failure, values of stress peaks must be considered. Using completely reverse equivalent stresses may lead to wrong conclusions. The corresponding constraint is given by

$$h_1(\mathbf{X}) = \sigma - \sigma_y < 0, \quad (37)$$

where σ_y is the yield stress and σ is a peak value of the stress.

The constraint function referred to the overall buckling of bars is given by

$$h_2(\mathbf{X}) = N_{xx} - \frac{\pi^2 EI}{l_e^2} < 0, \quad (38)$$

where I is the smallest moment of inertia of the cross section, E is the Young's modulus, l_e is the equivalent length and N_{xx} is the axial compressive load acting on the bar.

The constraint functions, considering local buckling on thin-walled box beams with rectangular cross section, are given by the following expressions (see Ref. [23]):

$$h_3(\mathbf{X}) = \sigma_y / [K_1 E (t/d)^2] - 1 \leq 0 \quad \text{and} \quad h_4(\mathbf{X}) = \sigma_y / [K_2 E (t/b)^2] - 1 \leq 0, \quad (39)$$

where t is the wall thickness, b and d are the width and height of the cross section and K_1 and K_2 are two dimensionless coefficients (values suggested by Iyengar and Gupta [23] for these coefficients are $K_1 = 21.72$ and $K_2 = 3.62$).

The constraint, when the probabilistic fatigue analysis has a fixed reliability index, may be written as

$$h_5(\mathbf{X}) = 1 - (\beta / \beta_{\text{fixed}}) \leq 0, \quad (40)$$

where β_{fixed} is the prescribed reliability index and β is the reliability index obtained with MCSIAS or FORM.

If the reliability analysis is carried out with FORM, using the limit state function given by Eq. (32), then an analytical expression for the reliability index β is obtained, which is given by Eq. (33). K and Δ are taken as random variables with lognormal probability distribution. In this case, for the optimization process, where a fixed value of β is adopted, the corresponding constraint may be obtained from Eqs. (33) and (40) as

$$h_5(\mathbf{X}) = 1 - \frac{\mu_{\ln LT}}{\ln LT_{\text{design}} - \beta_{\text{fixed}} \psi_{\ln LT}} \leq 0. \quad (41)$$

The value of $\mu_{\ln LT}$ is evaluated from the structural analysis for a specified number of samples. The fatigue curve is built with the mean value of K , and the total damage Δ , when fatigue failure occurs, is taken equal to 1.0 (which is a value commonly used).

6. A short description of the main program

The main program, taking into account the different subjects described in the previous sections, may be summarized as follows:

1. Define the problem characteristics.
2. If the optimization procedure will not be used, then calculate the reliability index with the FORM or MCSIAS described in Sections 4.2 and 4.3, respectively. The limit state function, LSF or $g(\mathbf{X})$, is given in Section 4.4, and the lifetime (LT) is evaluated carrying out the random dynamic fatigue analysis presented in Section 3.4.
3. If the optimization procedure will be used, then the method described in Section 5 is employed and the objective function to be minimized is the structural weight. As the constraints are independent of the random dynamic fatigue analysis and, optionally, from the reliability index, an iterative process (including subroutines performing the structural analysis and determining the reliability index) is necessary. When convergence is obtained, data with optimized dimensions are stored and step 2 is applied.

7. Numerical application

7.1. Model description

Algorithms presented in the previous sections are now applied to a hypothetical commercial vehicle, which is formed only by spatial frame elements. Welded joints, where several local effects may be considered, as well as constrained warping could be studied with more details using shell elements. However, in this case, it is necessary to analyze a very complex model, where the number of unknowns increases significantly with respect to a structure formed exclusively by frame elements.

The chassis is composed of two straight longitudinal beams and six straight transversal beams (with C-shaped cross sections), as indicated in Fig. 4, where the main dimensions are included.

The whole body is depicted in Fig. 5, while a side view, with the main dimensions of the body, is presented in Fig. 6. The set of bars forming the floor and linking the body to the chassis is shown in Fig. 7. The total number of bars and nodes are 254 and 461, respectively.

It is considered that the spatial frame elements are steel bars (ASTM A36) with the following characteristics: σ_y (yield stress) = 250 MPa, σ_r (ultimate stress) = 450 MPa, E (Young's modulus) = 2.06×10^5 MPa, G (shear modulus) = 7.92×10^4 MPa, ν (Poisson's ratio) = 0.3 and γ (specific weight) = 77 kN/m³.

The complete bus weighs 79 kN, but if passengers and baggage are included, the total weight increases to 123 kN, where 30.9 kN corresponds to the chassis and other fixed mechanical components. The weight of both axes (18.1 kN) have not been considered.

Pneumatic stiffness and damping are not considered, and the prescribed displacements induced by the road surface are directly applied to each axis. It is assumed that the mass of each axis does not generate inertial forces and that they do not have any influence. It is considered that the contact between each tire and the road is represented by a single point.

The suspension model is constituted by linear springs with stiffness coefficients equal to 300 kN/m. The shock absorbers are modeled as viscous damping mechanisms with a constant equal to 24.5 kNs/m corresponding to a damping ratio $\xi = 0.4$, which is a value commonly used in commercial vehicles [24].

7.2. Initial tests

The body was initially modeled using tubular bars with rectangular hollow cross sections characterized by the following dimensions: width = 0.04 m, height = 0.04 m and

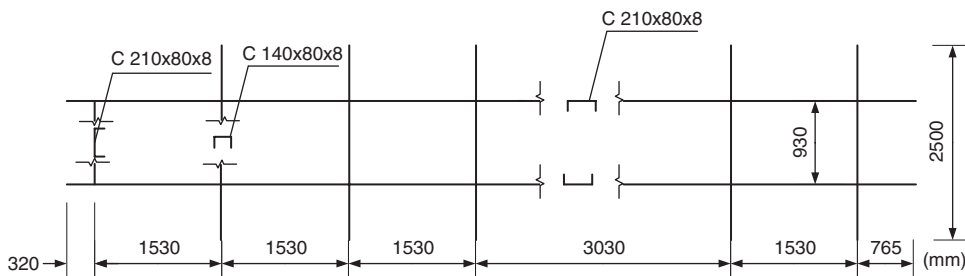


Fig. 4. Schematic representation of the chassis and its main dimensions (in mm).

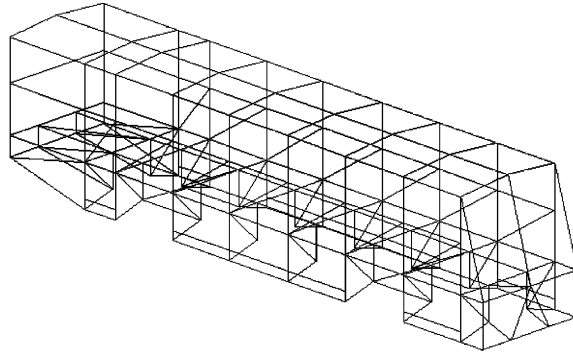


Fig. 5. Schematic representation of the body.

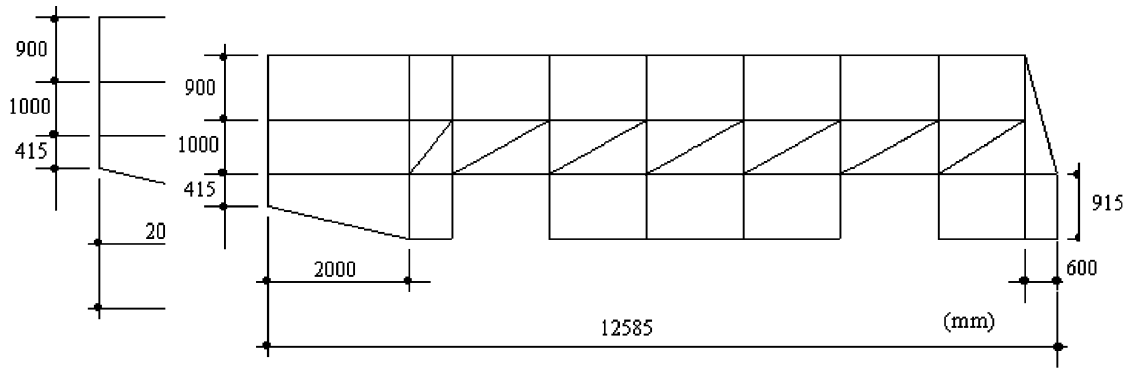


Fig. 6. Side view of the body with its main dimensions (in mm).

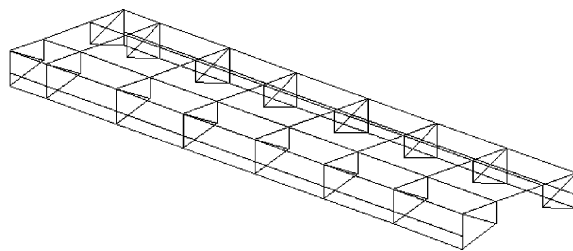


Fig. 7. Set of bars linking the body and the chassis.

thickness = 0.003 m. With this configuration, the weight of the frame structure corresponding to the body was 12.4 kN (here, weights of passengers, baggage, seats, water closet, etc., were not included).

The static analysis of the structure was carried out considering that the maximum load was acting on the vehicle, and the safety coefficients obtained for different bars were greater or equal to 4.0.

This structural configuration was also studied performing a random dynamic analysis, considering the vehicle velocity as equal to 25 m/s and with the pavement surface having a roughness coefficient $c = 40 \times 10^{-8}$, which is a common value used in secondary roads. The response stabilization in the adopted sample occurred in 2 s, and after this time, 8 s were used to carry out the dynamic analysis. A correlation coefficient of the parallel trails equal to 0.5 was assumed. The fatigue curve defined by EUROCODE 3 [18], extended for 2×10^8 cycles, and Shigley's method for multiaxial stress combination was adopted. The fatigue limit corresponding to 10^6 load cycles, for bars belonging to the body and the chassis were fixed in 154 MPa (the correction factors applied are $K_a = 0.89$, $K_b = 0.88$ and $K_{\text{weld}} = 0.875$) and 137 MPa (the correction factors applied are $K_a = 0.89$, $K_b = 0.78$ and $K_{\text{weld}} = 0.875$), respectively. Using standard curve "stress level vs. number of cycles" given by the EUROCODE 3 [18], the corresponding coefficients and cut-off limits are as follows:

- For the body:

$$m = 7.144, \quad a = 21.63, \quad K = 10^a = 4.24 \times 10^{21}, \quad 10^3 \leq N < 5 \times 10^6,$$

$$m = 9.144, \quad a = 25.81, \quad K = 10^a = 6.46 \times 10^{25}, \quad 5 \times 10^6 \leq N < 2 \times 10^8,$$

cut-off limit = 82.2 MPa.

- For the chassis:

$$m = 6.37, \quad a = 19.12, \quad K = 10^a = 4.14 \times 10^{19}, \quad 10^3 \leq N < 5 \times 10^6,$$

$$m = 8.37, \quad a = 23.67, \quad K = 10^a = 4.68 \times 10^{23}, \quad 5 \times 10^6 \leq N < 2 \times 10^8,$$

cut-off limit = 68.5 MPa.

For the random variables, the variation coefficients adopted here were $C_K = 0.08$ and $C_\Delta = 0.5$ (which is a very high value). In the lifetime estimation 10 samples were used and the coefficient C_θ was automatically calculated.

For this initial configuration a lifetime $LT = 2.08 \times 10^8$ s was obtained. Considering a design lifetime (which is the minimum value attributed to a desired lifetime) $LT_{\text{design}} = 1.3 \times 10^8$ s corresponding to a vehicle used during 10 years and working 10 h per day, the computed reliability index was $\beta = 0.43$, which is a very low value. The corresponding failure probability was 33.2 percent. Considering the same data applied to the previous case, but prescribing $C_\Delta = 0$, the corresponding computed reliability index was $\beta = 0.7$ (which is still a low value). Now considering the same data applied in the first case, but with the standard fatigue curve defined by EUROCODE 3 [18] and again using $C_\Delta = 0$, the corresponding computed reliability index was $\beta = 1.17$ (which corresponds to a failure probability equal to 11.5 percent). Observe that, for these three cases, the optimization procedure was not used and only one work condition for the vehicle was considered.

7.3. Optimization of the structural weight

To optimize the structural weight, bars were divided into three groups, based on constructive criteria. Each group may assume values of the cross sections that are available in Table 1.

The following conditions were established:

- (a) Elements belonging to group 1 are located at the floor of the vehicle, linking the body to the chassis. Numbers 2–9, indicated in Table 1, may identify the cross sections of these elements.
- (b) Elements belonging to group 2 are located at the sides of the vehicle. Numbers 1–7 may identify the cross sections of these elements, indicated in Table 1.
- (c) Elements belonging to group 3 are located at the roof of the vehicle. Numbers 1–7, indicated in Table 1, may identify the cross sections of these elements.

In order to apply the model to a more real situation, several work conditions for the vehicle, involving combinations of different kinds of pavement surfaces and different vehicle velocities, were established. These work conditions are shown in Table 2. The design lifetime LT_{design} was fixed in 3600 days, using the vehicle 10 h/day. For each simulation, 10 samples were used. A minimum value of the reliability index was fixed, and this value was taken as a constraint in the optimization procedure. The minimum value of the reliability index was $\beta_{\text{fixed}} = 3.0$.

The following results were obtained:

- (a) Cross sections:
 elements belonging to group 1: cross-section number 7;
 elements belonging to group 2: cross-section number 4;
 elements belonging to group 3: cross-section number 2.
- (b) Minimum value of the weight of the body structure: 14.4 kN (an increase of 2 kN with respect to the initial value). This value is related to two factors: (a) some severe work conditions were considered in Table 2 and (b) the value $\beta_{\text{fixed}} = 3.0$, which was adopted as a constraint in the

Table 1
Dimensions (in mm) of the available cross sections used as design variables

Cross section	Width	Height	Thickness
1	40	40	1.20
2	40	40	1.90
3	40	40	2.25
4	40	40	3.00
5	40	60	1.90
6	40	60	2.25
7	40	60	2.65
8	60	60	2.25
9	60	60	3.00
10	60	60	3.35
11	60	80	3.00
12	60	80	3.35

Table 2
Combination of different pavement surfaces and vehicle velocities

Road	Roughness coefficient c , Ref. [1]	Vehicle velocity (m/s)	Percentage for each work conditions (%)
Very good highway	15×10^{-8}	30.00	30
Average major road	30×10^{-8}	25.00	50
Average minor road	60×10^{-8}	15.00	15
Poor minor road	120×10^{-8}	11.11	5

optimization procedure, is really a very high value; this last aspect is more evident taking into account that $C_A = 0.5$ was taken, and this high value (suggestions of different authors vary from $C_A = 0.0$ until $C_A = 0.3$) influenced β , leading to lower values of the reliability index.

(c) Lifetime: 45,004 days, 10 h/day.

(d) Reliability index: $\beta = 3.15$ using FORM and $\beta = 3.18$ using MCSIAS.

(e) Computer process time: 36 h 13 min using a Pentium IV 3.2 GHz with 1 GB RAM DDR400, after 27 iterations in the optimization process. The code was written in fortran90.

7.4. Influence of the number of samples to estimate the lifetime

It is necessary to highlight that for the lifetime estimation, variability associated with several factors was found. If an ergodic process is considered, the lifetime estimation is obtained from data corresponding only to one sample. However, each sample has its own number of cycles and stress levels resulting from the cycle counting process. In each stress cycle, Eq. (11) or (13) is applied, where the coefficient m may take different values, such as those given previously in this example, depending on the part of the fatigue curve that is considered. Consequently, a significant variability to estimate the lifetime is verified. For example, the frame structure obtained from the optimization procedure described in the previous section was considered. Table 3 shows the lifetime (in days) and the reliability index β , calculated with $C_\theta = 0$ and 0.75, corresponding to ten samples. Values of the reliability index were computed using Eqs. (33) and (34). The mean value and the standard deviation of the lifetime and the mean value of the reliability index were also included in the same table (this last value is not a mean of values contained in the reliability index column of Table 3, it was calculated using the mean value and the standard deviation of the lifetime in Eq. (33)). The value of the coefficient $C_\theta = \psi_{\ln LT} / \mu_{\ln LT} = 0.75$ is very high (although a value of C_θ equal to 0.45 was reported by Wirsching [5]). It is expected that taking more than ten samples, the value of C_θ will be less than 0.75.

7.5. Some important remarks

In this example, 200 harmonic components were used to simulate in the time domain the road roughness and the corresponding prescribed displacement. This number of harmonic components was necessary to represent, with a very small error (less than 1 percent), the area of the spectral

Table 3
Lifetime estimation (in days) for 10 samples considering a vehicle working 10 h/day

Sample	Lifetime (days)	Reliability index (β) ^a	
		$C_\theta = 0.00$	$C_\theta = 0.75$
1	68,654	6.49	3.63
2	22,123	4.00	2.22
3	88,889	7.06	3.95
4	16,089	3.31	1.85
5	11,901	2.63	1.47
6	19,663	3.74	2.09
7	87,204	7.02	3.92
8	88,889	7.06	3.95
9	14,752	3.36	1.88
10	31,882	4.79	2.68
Mean	45,004	5.61	3.18
Standard deviation	33,955		

^aValues of β were obtained considering the variation coefficient C_θ , obtained from the ten samples, dividing the standard deviation of the lifetime by the mean value.

density function and the whole process in terms of its statistics (mean value and standard deviation).

Factors such as the time when the structural response is stabilized and the time interval adopted in a specific sample to estimate the lifetime have not shown relevant influences.

8. Final remarks

A time domain approach to deal with fatigue effects due to pavement roughness on commercial vehicle structures was presented in this work. A versatile computational code was formulated to estimate the vehicle lifetime and to determine, alternatively, the respective reliability index. Structural weight optimization for a specified vehicle lifetime with a prescribed reliability index was also included.

In order to get a good computational performance, it would be necessary to consider an ergodic process, where a unique sample is representative of the complete process. However, preliminary tests have shown significant variations in the lifetime among the different samples, due to the sensibility associated with fatigue analysis and due to the cycles counting process with the rainflow method. Therefore, it seems necessary to work with many samples sacrificing the computational performance.

Looking for a good approximation of the results with respect to the real situation, a correct representation of the different pavement characteristics and vehicle velocity levels (including the time spent by each of these velocity levels) is necessary. Determination of the vehicle lifetime, the reliability index and the optimal weight is strongly dependent on specifications with respect to the form of the vehicle that has been used.

In fatigue problems, where a high variability of parameters and results may be found, reliability analysis has a very important role to play. In the computational code, based on the algorithms described previously, the reliability index may be determined using MCSIAS or, alternatively, FORM. However, the most important aspect is the definition of the random variables and their respective distribution probability function. A closed solution for the reliability index, using FORM, was used in this work, improving the computational performance.

Farkas' algorithm, used to optimize the structural weight, has shown to be a very robust method, but too many iterations were necessary to obtain the desired convergence.

The fact that the reliability index may be used as a constraint in the optimization process emphasizes the importance of the computational code as an auxiliary tool for vehicle structural analysis and design.

Acknowledgments

The authors wish to thank FAPERGS, CAPES and CNPq (Brazilian Research Councils) for their financial support.

References

- [1] C.J. Dodds, J.D. Robson, The description of road surface roughness, *Journal of Sound and Vibration* 31 (1973) 175.
- [2] S.C. Ashmore, H.C. Hodges, Dynamic force measurement vehicle (DFMV) and its application to measuring and monitoring road roughness, *Vehicle, Tire, Pavement Interface*, ASTM, Philadelphia, 1992, pp. 1–13, STP 1164.
- [3] R.W. Clough, J. Penzien, *Dynamics of Structures*, 2nd ed., McGraw-Hill, New York, 1993.
- [4] K.J. Bathe, *Finite Element Procedures In Engineering Analysis*, Prentice Hall, Englewood Cliffs, NJ, 1996.
- [5] P.M. Wirsching, Probabilistic fatigue analysis, in: C. Sundararajan (Ed.), *Probabilistic Structural Mechanics Handbook*, Chapman & Hall, New York, 1995, pp. 146–165 (Chapter 7).
- [6] J.A. Collins, *Failure in Materials in Mechanical Design*, 2nd ed., Wiley, New York, 1993.
- [7] A. Haldrar, S. Mahadevan, *Reliability Assessment Using Stochastic Finite Element Analysis*, Wiley, New York, 2000.
- [8] U. Bourgund, C.G. Bucher, *Importance Sampling Procedures Using Design Points—a User Manual*, Institute of Engineering Mechanics, University of Innsbruck; Report no. 8-86, Innsbruck, Austria, 1986.
- [9] H.O. Madsen, S. Kren, N.C. Lind, *Methods of Structural Safety*, Prentice-Hall, Englewood Cliffs, NJ, USA, 1986.
- [10] R.E. Melchers, *Structural Reliability and Predictions*, Ellis Horwood, London, UK, 1997.
- [11] P. Bjerager, Probability interpretation by directional simulation, *Journal of Structural Engineering (ASCE)* 110 (8) (1987) 1707–1724.
- [12] C.S. Bucher, Adaptive sampling—an iterative fast Monte Carlo procedure, *Structural Safety* 5 (1988) 119–126.
- [13] G.I. Schuëller, C.G. Bucher, U. Bourgund, W. Ouypornprasert, An efficient computational scheme to calculate structural failure probabilities, *Probabilistic Engineering Mechanics* 4 (1) (1989).
- [14] J. Farkas, *Optimum Design of Metal Structures*, Ellis Horwood Limited, Chichester, UK, 1984.
- [15] R.L. Norton, *Machine Design*, Prentice-Hall, Englewood Cliffs, NJ, 1998.
- [16] R.C. Juvinall, *Fundamentals of Machine Component Design*, Wiley, New York, 1983.
- [17] J.E. Shigley, *Mechanical Design*, McGraw Hill, New York, 1963.
- [18] EUROCODE 3: Design of Steel Structures, Part 1.1, European Committee for Standardization, Brussels, Belgium, 1993.
- [19] H.O. Fuchs, R.I. Stephens, *Metal Fatigue in Engineering*, Wiley, New York, 1980.

- [20] P.L. Liu, A. Der Kiureghian, Multivariate distribution models with prescribed marginal covariance, *Probabilistic Engineering Mechanics* 1 (2) (1986) 105–112.
- [21] H.M. Gomes, A.M. Awruch, Reliability of reinforced concrete structures using stochastic finite elements, *Engineering Computations* 19 (7) (2002) 764–786.
- [22] P.M. Wirsching, Y.N. Chen, Consideration of probability based fatigue design criteria for marine structures, *Marine Structures* 1 (1988) 23–45.
- [23] N.G.R. Iyengar, S.K. Gupta, *Programming Methods In Structural Design*, Edward Arnold, London, 1980.
- [24] T.D. Gillespie, *Fundamentals of Vehicle Dynamics*, SAE, Warrendale, 1992.